Heat capacity of the discotic mesogen, 2,3,6,7,10,11-hexa-n-hexyloxytriphenylene, between 17 and 397 K and phase transitions in the solid and liquid states

Michio Sorai[a]; Shuichi Asahina[ab]; Christian Destrade[b]; Nguyen Huu Tinh[c]

[a] Chemical Thermodynamics Laboratory, Faculty of Science, Osaka University, Osaka, Japan [b] Centre de Recherche Paul Pascal, Domaine Universitaire, Talence, Cedex, France [c] Industrial Institute of Tottori Prefecture, Yonago, Tottori

PLEASE SCROLL DOWN FOR ARTICLE

Heat capacity of the discotic mesogen, 2,3,6,7,10,11-hexa-*n*-hexyloxytriphenylene, between 17 and 397 K and phase transitions in the solid and liquid states†

by MICHIO SORAI and SHUICHI ASAHINA‡

Chemical Thermodynamics Laboratory, Faculty of Science, Osaka University, Toyonaka, Osaka 560, Japan

CHRISTIAN DESTRADE and NGUYEN HUU TINH

Centre de Recherche Paul Pascal, Domaine Universitaire, 33405 Talence Cedex, France

The heat capacity of the discotic mesogen, 2,3,6,7,10,11-hexa-*n*-hexyloxytriphenylene whose purity was better than 99·3 mole per cent has been measured with an adiabatic calorimeter between 17 and 397 K. Five solid–solid phase transitions were observed in the crystalline state at 105·90, 220·86, 233·91, 330·81, and 337·10 K. The melting and clearing points were 340·27 and 371·17 K, respectively. The sum of all of the solid-to-solid phase transition entropies amounted to 44·87 J K^{-1} mol^{-1} (25·8 per cent of the total transition entropy). These solid–solid phase transitions can be ascribed to successive conformational melting of the alkyl-chains attached to the central triphenylene core. The present result strongly supports the prediction that a rich solid polymorphism is a necessary condition for favourable formation of the columnar structure in the discotic mesophases. The entropy change at the phase transition from the columnar mesophase to the isotropic liquid was very small in comparison to that observed for the discotic mesogens having a benzene core. This small transition entropy is discussed in relation to the wider temperature range for the discotic mesophase in the triphenylene derivatives compared to the benzene-core mesogens. Thermal properties of the discotic mesogens are compared to those of classical rod-like liquid crystals.

1. Introduction

Since the discovery of the new mesophase formed by disc-shaped molecules [1], various discotic mesogens have been found [2–14]. Apart from the discotic nematic [15] and cholesteric phases [16], all the discotic phases are columnar phases with the molecules stacked in columns [1, 9, 11, 14, 17]. This structural feature is in sharp contrast to classical liquid crystals consisting of rod-like molecules. However, the discotic mesophases can never be realized from pure disc-shaped molecules such as condensed polycyclic aromatics [18]. The 'disc-shaped' molecules capable of forming the discotic mesophases generally have structures in which flexible alkyl-chains are bonded directly or through ether- or ester-linkages to an aromatic central core. The intermolecular forces responsible for formation of the columnar structures in the

discotic mesophases are van der Waals interaction of the π-electrons of the central cores, dipole–dipole interaction between the bond moments locally existing in the molecules [19], and intermolecular hydrogen bonding [20]. In fact, disc-like molecules having big aromatic cores such as triphenylene or truxene exhibit the columnar mesophases over a wider temperature range than those having small aromatic cores such as benzene. Likewise, when the $-OCOC_nH_{2n+1}$ side-chains are partially replaced by $-NHCOC_nH_{2n+1}$ groups which have a stronger bond moment and are capable of forming intermolecular hydrogen bondings, intermolecular interactions in a column are strengthened. Consequently, the thermal stability of the discotic mesophase is enhanced and the temperature range for the mesophase becomes dramatically wider [21].

In addition, one may ask what role do the flexible chains play in the formation of the various discotic mesophases? On the basis of heat capacity measurements and infrared absorption study on the discotic mesogens of hexa-substituted benzene [22–25] and triphenylene derivative [26], we have demonstrated that conformational melting of the alkyl-chains in the solid state seems to be a necessary condition for formation of the columnar discotic mesophases. Unlike the classical liquid crystals, the discotic mesogens so far studied by calorimetry always exhibit a rich solid polymorphism. Thus it is concluded that conformational melting of the alkyl-chains proceeds, remarkably, even in the solid state. In other words, discotic mesogens exist in a highly disordered crystalline phases prior to appearance of their columnar mesophases. The degree of disorder can be related to the entropy increase at each phase transition. Microscopic evidences for the conformational melting of the alkyl-chains in the solid state have been provided by solid-state ^2H N.M.R. [27, 28] and ^{13}C N.M.R. [27, 29].

We report here the results of adiabatic calorimetry on the discotic mesogen, 2,3,6,7,10,11-hexa-*n*-hexyloxytriphenylene, herein called C6-HET. This mesogen is well suited for the calorimetric study for two reasons. First, since this compound is hexa-substituted *ether* of triphenylene, one can learn the importance of ether alkyl-chains in the formation of the discotic mesophase compared to the hexa-substituted *ester* of benzene [22–25] and triphenylene [26]. Second, since the columnar mesophase of this mesogen persists over a wide temperature range, from 68 to 97°C [4], the thermal properties of the discotic mesophase itself can easily be examined. This is an important factor since in the case of benzene-hexa-*n*-alkanoates, the mesophase range was so narrow as 5·5°C or less [1, 5] that comparison of the heat capacities of the discotic mesophase with those of the solid and isotropic phases involved more than desired uncertainty [22–25].

2.   Experimental

The material, C6-HET, whose molecular formula is schematically drawn in figure 1, was prepared according to the method previously described [4]. The sample was purified by chromatography on silica gel using a mixture of benzene and hexane (50/50) as eluant and recrystallized from absolute ethanol.

Variable temperature infrared spectra in the range 4000 $\sim$ 400 cm^{-1} were recorded for Nujol mulls with an Infrared Spectrophotometer Model DS-402G (Japan Spectroscopic Co., Ltd.).

Textures of the phases above room temperature were observed by a polarizing microscope Model BHA-751-P (Olympus) equipped with a heating stage (Union Optical Co., Ltd., Model CMS-2).
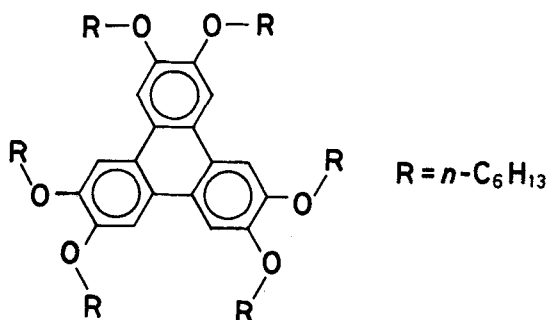
Figure 1.   Molecular formula of 2,3,6,7,10,11-hexa-*n*-hexyloxytriphenylene (C6-HET).

Heat capacities in the range from 17 to 397 K were measured with a new adiabatic calorimeter [30]. The calorimeter cell was specifically made for the sake of the present sample. It was made of gold-plated copper container and beryllium copper lid, and had inner volume of $6\,\mathrm{cm}^3$. Temperature of the calorimeter cell was measured with a platinum resistance thermometer (Minco Products, Inc., Model S1059-2, nominal $100\,\Omega$) whose temperature scale had been calibrated on the basis of the IPTS-68. The cell was filled to 80 per cent of its total volume by repeating a load-melt-freeze-load cycle of sample addition under atmosphere of helium gas. The amount of sample charged was $0.0052349\,\mathrm{mol}(=4.3411\,\mathrm{g}$ after a buoyancy correction assuming a sample density of $1.12\,\mathrm{g\,cm}^{-3})$. Helium gas (400 Torr) was sealed in the cell to aid the heat transfer.

3.   Results

Calorimetric results are evaluated in terms of molar heat capacities under constant pressure, C_p. Strictly speaking, correction for vaporization of the sample into the free space of the calorimeter cell should be made for heat capacities of the liquid state. However, since the free space is as small as $\sim 1\,\mathrm{cm}^3$ and the vapour pressure seems to be very small, we neglected this correction. The molar heat capacities of C6-HET in the whole temperature region investigated here are listed in Table 1 and plotted in figure 2.

Five phase transitions were observed in the crystalline state at 105·90, 220·86, 233·91, 330·81, and 337·10 K. In what follows, the six phases are designated as Phases I, II, III, IV, V and VI, respectively, in going from high to low temperatures. The melting point was $T_\mathrm{m} = 340.27\,\mathrm{K}$ while the clearing point corresponding to the phase transition from the columnar mesophase to the isotropic liquid was $T_\mathrm{C} = 371.17\,\mathrm{K}$. These two phases are designated in figure 2 as 'D' and 'IL', respectively. The melting and clearing temperatures agree well with the 341 and 370 K observed by DSC [4]. The phase bounded by two temperatures (340·27 and 371·17 K) was previously assigned to a liquid crystalline columnar phase [4]. When the sample was cooled from the isotropic liquid to the columnar mesophase, a focal-conic texture was observed under a polarizing microscope (see figure 3). This columnar mesophase has been classified as a D_ho phase in which the molecules are regularly stacked in the columns with hexagonal lattice [14, 31].

An amazing result is the fact that the C_p peak at 337·10 K arising from the phase transition from Phase II to I is located very close to the melting peak at 340·27 K. We first thought this close peak was due to contamination by impurities capable of forming eutectic mixtures. In such a case one can expect a heat capacity anomaly as demonstrated by the present study, particularly when the impurities have molecular structures similar to a host molecule. We used liquid chromatography to
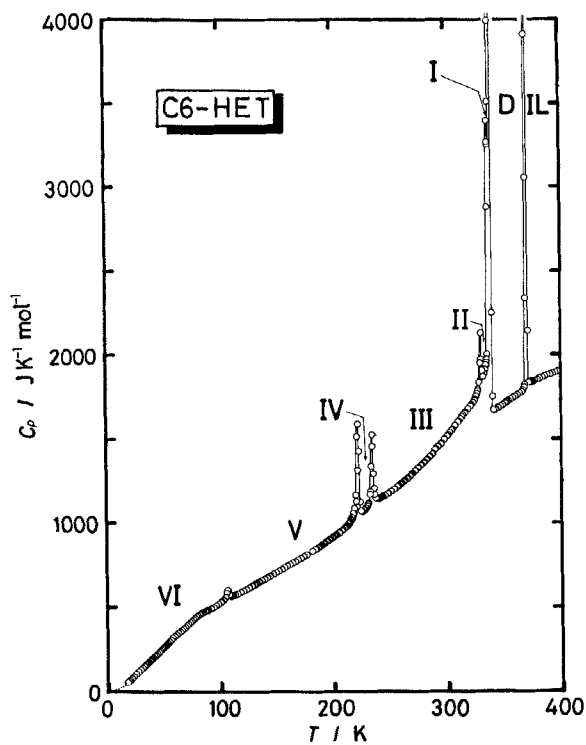
M. Sorai *et al.*

Figure 2.   Molar heat capacity of C6-HET in the range from 17 to 397 K. The crystalline
phases are indicated by I, II, III, IV, V, and VI while the discotic columnar mesophase
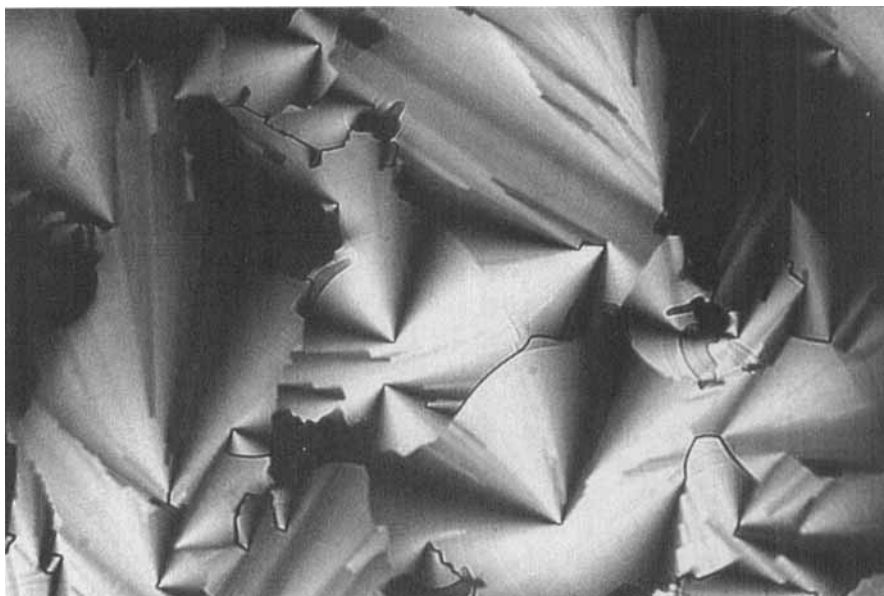and isotropic liquid phase are labelled by 'D' and 'IL', respectively.

Figure 3.   The focal-conic texture of the columnar mesophase of C6-HET observed on
cooling: magnification 100 ×.

Table 1. Molar heat capacity of C6-HET: relative molecular mass 829·257.

$\dfrac{T}{K}$	$\dfrac{C_p}{JK^{-1}\,mol^{-1}}$	$\dfrac{T}{K}$	$\dfrac{C_p}{JK^{-1}\,mol^{-1}}$	$\dfrac{T}{K}$	$\dfrac{C_p}{JK^{-1}\,mol^{-1}}$
			Series 1		
188·539	858·74	199·540	911·94	210·127	972·34
191·336	872·00	202·223	925·88	212·706	992·72
194·098	885·67	204·883	940·43	215·253	1019·1
196·832	898·87	207·517	955·72		
			Series 2		
125·107	614·49	154·258	722·10	179·032	824·43
127·917	625·51	156·747	732·21	181·548	830·00
130·689	635·35	159·214	741·86	184·048	840·32
133·426	645·84	161·660	750·77	186·528	850·69
136·130	655·85	164·085	760·24	188·990	861·45
138·803	665·70	166·489	768·39	191·433	872·32
141·446	675·41	168·875	779·19	193·857	883·36
144·060	685·04	171·360	788·80	196·263	894·86
146·648	694·52	173·943	799·12	198·650	906·66
149·209	703·83	176·495	808·15	201·018	918·49
151·745	713·43				
			Series 3		
82·106	458·15	93·640	498·14	105·109	579·77
84·515	467·92	95·814	506·54	107·713	570·37
86·867	475·73	97·950	515·00	110·307	563·45
89·169	482·72	100·049	524·51	112·877	570·60
91·426	490·28	102·448	538·64		
			Series 4		
17·754	52·69	19·758	67·28	20·697	73·96
18·780	60·56				
			Series 5		
29·034	124·60	49·582	259·13	70·110	389·54
30·989	138·57	50·575	264·97	71·588	398·17
32·880	151·41	51·539	270·98	73·031	407·21
34·591	162·90	52·474	277·39	74·442	415·99
36·164	173·25	53·383	283·86	75·823	424·55
37·625	183·16	54·633	294·01	77·176	432·81
38·994	191·83	56·187	305·44	78·504	441·26
40·286	200·78	57·755	316·74	79·808	448·26
41·576	208·86	59·338	327·16	81·091	454·80
42·868	216·81	60·868	336·42	82·355	460·36
44·099	224·08	62·350	344·90	83·602	465·30
45·279	231·91	63·853	353·45	84·880	469·87
46·412	239·65	65·437	362·41	86·189	473·52
47·504	246·64	67·038	371·78	87·482	478·33
48·560	252·71	68·594	380·59	88·760	481·26
			Series 6		
20·152	66·54	29·279	127·34	36·288	174·14
21·805	76·71	30·920	138·18	37·430	181·90
23·425	87·77	32·415	148·41	38·514	188·90
25·351	102·07	33·794	157·72	39·549	195·95
27·447	116·58	35·080	166·18		

M. Sorai *et al.*

Table 1 (*continued*).

$\dfrac{T}{\text{K}}$	$\dfrac{C_p}{\text{JK}^{-1}\,\text{mol}^{-1}}$	$\dfrac{T}{\text{K}}$	$\dfrac{C_p}{\text{JK}^{-1}\,\text{mol}^{-1}}$	$\dfrac{T}{\text{K}}$	$\dfrac{C_p}{\text{JK}^{-1}\,\text{mol}^{-1}}$
		Series 7			
100·662	527·96	104·194	555·86	108·357	564·52
102·310	536·74	106·287	597·07	110·435	564·07
		Series 8			
102·454	536·11	115·074	576·75	131·954	637·91
104·204	554·25	117·578	585·74	134·256	646·32
105·903	596·80	120·048	594·70	136·535	654·82
107·581	571·56	122·486	603·23	138·792	663·18
109·262	560·62	124·894	611·85	141·027	671·55
110·935	567·49	127·274	620·66	143·447	680·43
112·793	569·45	129·626	629·20		
		Series 9			
199·895	911·12	210·988	976·02	216·669	1023·6
202·264	924·16	212·136	983·56	217·782	1045·5
204·615	937·72	213·279	993·04	218·887	1070·8
206·948	951·23	214·416	1001·7	219·971	1124·4
209·261	965·80	215·546	1011·7	221·002	1308·4
		Series 10			
226·254	1075·0	237·536	1141·0	250·304	1184·3
228·224	1084·9	239·446	1139·4	253·091	1198·1
230·179	1108·1	241·353	1144·6	255·857	1212·7
232·089	1185·4	243·253	1151·9	258·603	1227·6
233·870	1455·1	245·146	1159·6	261·328	1242·4
235·650	1202·7	247·498	1170·9		
		Series 11			
269·032	1288·5	289·650	1434·8	313·284	1629·4
271·677	1304·9	292·097	1453·0	316·255	1652·8
274·306	1321·4	294·885	1468·6	319·202	1675·7
276·919	1338·6	298·017	1497·8	322·126	1699·7
279·515	1356·1	301·126	1523·0	325·024	1726·7
282·091	1374·1	304·208	1550·1	327·883	1781·9
284·644	1391·7	307·262	1578·3	330·636	1969·1
287·168	1408·2	310·287	1605·5		
		Series 12			
257·260	1220·6	262·713	1251·8	268·073	1283·3
259·977	1235·7	265·405	1266·3		
		Series 13			
185·131	842·87	277·759	1342·6	340·045	50130
187·611	853·86	280·345	1360·3	340·080	57201
190·073	865·19	282·909	1378·1	340·117	65286
192·515	876·22	285·449	1395·1	340·138	72758
194·939	887·46	287·957	1413·1	340·163	80953
197·345	898·84	290·420	1439·1	340·185	89487
199·732	911·57	292·859	1453·7	340·206	95683
202·098	923·47	295·313	1471·6	340·225	100082
204·447	935·65	297·766	1495·0	340·244	107542
206·776	949·81	300·203	1515·8	340·261	110492
209·086	964·56	302·622	1536·2	340·282	79301
211·582	977·73	305·027	1556·2	340·564	2249·2

Table 1 (*continued*).

$\dfrac{T}{\text{K}}$	$\dfrac{C_p}{\text{JK}^{-1}\text{mol}^{-1}}$	$\dfrac{T}{\text{K}}$	$\dfrac{C_p}{\text{JK}^{-1}\text{mol}^{-1}}$	$\dfrac{T}{\text{K}}$	$\dfrac{C_p}{\text{JK}^{-1}\text{mol}^{-1}}$
212·712	988·28	307·417	1577·5	341·150	1748·1
213·856	998·82	309·789	1598·8	341·950	1672·2
214·991	1009·7	312·142	1619·6	343·456	1674·1
216·116	1029·6	314·477	1640·2	345·492	1682·6
217·233	1053·1	316·799	1657·5	347·521	1691·9
218·337	1082·9	319·109	1675·1	349·544	1700·1
219·413	1163·3	321·406	1692·7	351·560	1709·3
220·402	1511·6	323·686	1713·7	353·569	1718·4
221·309	1587·0	325·293	1733·4	352·543	1716·4
222·232	1425·7	326·238	1751·0	354·541	1724·8
223·244	1122·1	327·180	1765·9	356·532	1733·1
224·331	1067·7	328·115	1790·3	358·521	1742·0
225·431	1063·2	329·040	1833·0	360·505	1749·4
226·531	1067·9	329·943	1946·0	362·482	1758·8
227·628	1075·3	330·806	2127·9	364·453	1766·7
228·720	1084·9	331·676	1902·5	366·417	1776·6
229·806	1096·7	332·580	1865·4	368·367	1804·2
230·884	1115·8	333·485	1883·0	370·032	3052·1
231·945	1167·4	334·386	1909·0	370·840	5356·8
232·960	1334·0	335·279	1936·1	371·060	5838·0
233·905	1524·0	335·061	1935·4	371·272	5877·8
234·860	1289·8	335·506	1949·8	371·500	4910·2
235·882	1165·5	335·948	1969·5	371·841	2142·8
236·936	1141·9	336·387	2000·7	372·300	1833·8
237·996	1138·2	336·778	2877·4	372·782	1834·2
239·057	1139·2	337·104	3391·6	373·263	1836·0
240·116	1142·1	337·416	3263·2	374·224	1834·0
241·174	1145·4	337·732	3247·7	374·706	1837·1
242·229	1149·1	338·041	3508·7	375·186	1841·2
242·231	1154·9	338·327	3990·5	375·665	1841·3
245·224	1159·2	338·585	4627·3	376·145	1835·2
248·048	1172·3	338·814	5440·5	377·472	1844·6
250·853	1185·5	339·013	6500·8	379·643	1848·2
253·638	1199·5	339·208	8075·6	381·811	1855·6
256·402	1214·0	339·393	10341	383·974	1861·3
259·145	1228·9	339·543	13164	386·132	1868·6
261·867	1244·2	339·663	16655	388·283	1874·4
264·567	1259·3	339·760	20618	390·722	1878·9
267·243	1275·5	339·839	26391	392·867	1884·2
269·897	1291·9	339·903	31559	395·003	1890·4
272·533	1308·0	339·958	36616	397·130	1896·3
275·154	1324·9	340·005	43374		

check for such impurities. The resulting purity was 99·8 mole per cent or better. In addition, we determined the sample purity based on the calorimetric fractional melting method by use of the single melting peak at 340·27 K. The result was 99·3 mole per cent. When experimental errors are taken into account, we can conclude that the present specimen does not contain sufficient impurities to cause the heat capacity peak at 337·10 K. Hence, the peak at 337·10 K can reasonably be assigned to a solid-to-solid phase transition, i.e. the transition from Phase II to I.

To obtain the excess heat capacities of these phase transitions from the observed values, we estimated the so-called 'normal heat capacity' curves as follows. For the
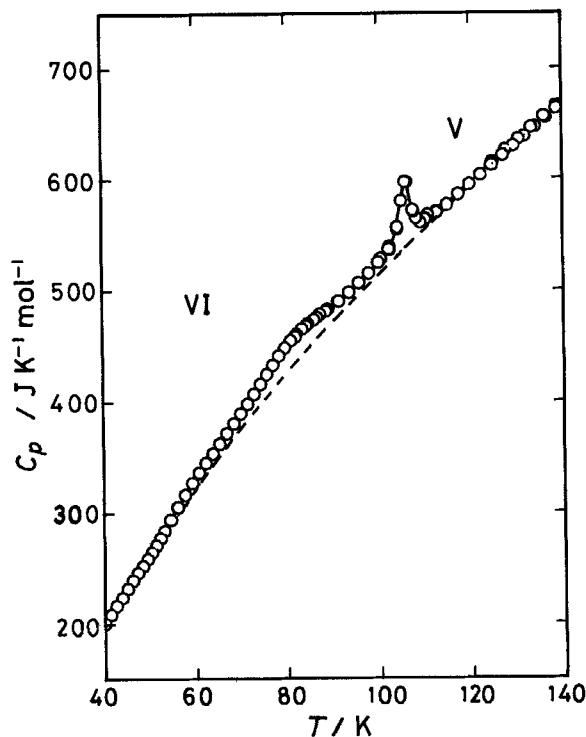
Figure 4.   Molar heat capacity of C6-HET in the vicinity of the phase transition from Phase
VI to V. The broken curve corresponds to the normal heat capacity.

transition between Phases VI and V, an effective frequency-distribution method [32]
was adopted. Normal heat capacity principally consists of contributions from a
continuous phonon distribution arising from the acoustic modes and many discrete
intramolecular vibrations due to the optical modes. The latter contribution can be
well approximated by the Einstein model in which the characteristic frequencies
correspond to the fundamental bands detected by I.R. and/or Raman spectroscopy.
Since all of the normal modes of intramolecular vibrations are not always observed
by I.R. and Raman spectroscopy, the contribution from these intramolecular vibra-
tions not detected spectroscopically was effectively included in the continuous spec-
trum of the acoustic modes. By using the C_p values in the ranges 20–50 K and
130–180 K, the 'best' effective frequency distribution below 700 cm^{-1} was determined
through a computer-fitting. The normal heat-capacities thus obtained for the inter-
polated region from 50 to 130 K are shown in figure 4 by a broken curve. Moreover,
extrapolation of this normal heat-capacity curve to 0 K enables us to evaluate
the standard thermodynamic functions of C6-HET. Table 2 lists the heat capacity
C_p°, molar entropy S°, enthalpy function $(H^\circ - H_0^\circ)/T$, and the Gibbs function
$-(G^\circ - H_0^\circ)/T$ at rounded temperatures.

For both the phase transitions from Phase V to IV and from Phase IV to III, we
adopted a common single curve represented by a cubic equation with respect to
temperature (see figure 5).

The normal heat capacities for the phase transitions from Phase III to II, II to I,
and the melting (from Phase I to D) were approximated by two straight lines
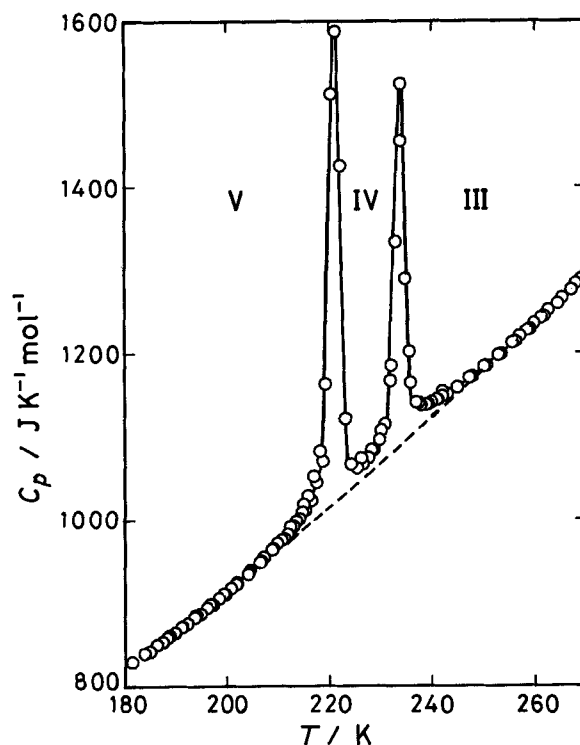
Figure 5. Molar heat capacity of C6-HET in the vicinity of the phase transitions from Phase V to IV and IV to III. The broken curve represents the normal heat capacity.

illustrated in figure 6. The straight line in the solid state was determined by use of eight C_p data in the range from 260 to 280 K. These two straight lines have been connected vertically at the melting temperature. As a result, the normal heat capacity dropped by $80 \, \text{J K}^{-1} \, \text{mol}^{-1}$ from 1740 to $1660 \, \text{J K}^{-1} \, \text{mol}^{-1}$ at the melting point. As discussed in the next section, small heat capacity of the columnar mesophase in comparison with that of the crystal phase is a characteristic feature of the discotic mesogens so far studied calorimetrically [23–26].

The normal heat capacities for the phase transition from the columnar mesophase to the isotropic liquid were approximated by two straight lines shown in figure 7. In this case, two base lines are connected vertically at the clearing point to give a jump of $28 \, \text{J K}^{-1} \, \text{mol}^{-1}$ from $1795 \, \text{J K}^{-1} \, \text{mol}^{-1}$ of the columnar mesophase to $1823 \, \text{J K}^{-1} \, \text{mol}^{-1}$ of the isotropic liquid. Here again, low heat-capacity of the columnar mesophase compared with that of the isotropic liquid is a remarkable inherent property of the discotic mesogens [23–26].

The difference between the observed and normal heat capacities is the excess heat capacity ΔC_p due to the phase transitions. The enthalpy (ΔH) and entropy (ΔS) arising from the phase transitions were determined by integration of ΔC_p with respect to T and $\ln T$, respectively. The ΔH and ΔS thus determined are listed in table 3.

Table 2. Standard thermodynamic functions for C6-HET in $J\,K^{-1}\,mol^{-1}$. The values in the parentheses are extrapolated.

T/K	C_p°	S°	$(H^\circ - H_0^\circ)/T$	$-(G^\circ - H_0^\circ)/T$
5	(1·50)	(0·501)	(0·376)	(0·125)
10	(11·79)	(3·986)	(2·985)	(1·000)
15	(34·73)	(12·730)	(9·436)	(3·294)
20	95·50	26·872	19·612	7·260
30	132·10	66·082	46·056	20·027
40	198·91	113·255	75·925	37·329
50	261·59	164·396	106·812	57·583
60	331·16	218·234	138·413	79·821
70	388·89	273·622	170·090	103·532
80	449·24	329·528	201·243	128·285
90	485·50	384·752	231·010	153·742
100	524·29	437·790	258·307	179·484

Phase transition (VI → V) at 105·90 K

T/K	C_p°	S°	$(H^\circ - H_0^\circ)/T$	$-(G^\circ - H_0^\circ)/T$
120	594·53	543·220	311·649	231·571
140	667·70	640·313	357·219	283·094
160	744·72	734·544	400·894	333·650
180	826·57	826·778	443·445	383·333
200	912·92	917·930	485·701	432·230
220	1370·2	1011·794	531·208	480·587

Phase transition (V → IV) at 220·86 K

Phase transition (IV → III) at 233·91 K

T/K	C_p°	S°	$(H^\circ - H_0^\circ)/T$	$-(G^\circ - H_0^\circ)/T$
240	1141·8	1116·602	587·238	529·364
260	1233·8	1211·283	633·112	578·170
280	1358·0	1307·084	680·286	626·798
298·15	1498·3	1396·546	725·628	670·919
300	1514·2	1405·864	730·443	675·421
320	1682·0	1509·050	784·767	724·283

Phase transition (III → II) at 330·81 K

Phase transition (II → I) at 337·10 K

T/K	C_p°	S°	$(H^\circ - H_0^\circ)/T$	$-(G^\circ - H_0^\circ)/T$
340	42706·0	1674·256	900·474	773·782

Phase transition (I → mesophase) at 340·27 K

T/K	C_p°	S°	$(H^\circ - H_0^\circ)/T$	$-(G^\circ - H_0^\circ)/T$
360	1747·5	1835·863	1005·815	830·048

Phase transition (mesophase → liquid) at 371·17 K

T/K	C_p°	S°	$(H^\circ - H_0^\circ)/T$	$-(G^\circ - H_0^\circ)/T$
380	1849·5	1947·293	1061·411	885·882
390	1877·6	1995·725	1082·006	913·719

4. Discussion

4.1. *Phase transitions in the solid and liquid states*

As seen from figure 2 and table 3, the present discotic mesogen C6-HET exhibited a rich solid polymorphism. Judging from the analogy of the related compounds [22–29, 33, 34], the origin of the solid phase transitions is surely the partial
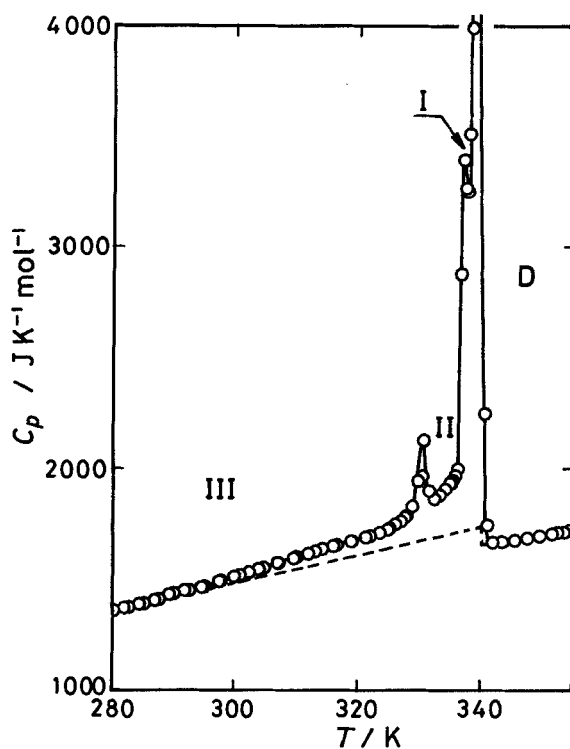
Figure 6. Molar heat capacity of C6-HET in the vicinity of the phase transitions from Phase III to II, II to I, and I to the mesophase (the melting). The broken line shows the normal heat capacity.

Table 3. Enthalpy and entropy of phase transitions in C6-HET.

Transition	T_{trs}/K	$\Delta H/kJ\,mol^{-1}$	$\Delta S/J\,K^{-1}\,mol^{-1}$	
Phase VI → V	105·90	1·16	13·43	
Phase V → IV	220·86	1·95	5·56	
Phase IV → III	233·91	1·30	8·83	44·87
Phase III → II	330·81	3·06	9·59	(25·8%)
Phase II → I	337·10	2·51	7·46	
Phase I → D	340·27	39·05	114·91	(66·1%)
Phase D → IL	371·17	5·24	14·13	(8·1%)
			Total 173·91	(100%)

conformational melting of the alkyl-chains attached to the central triphenylene core. The sum of the transition entropies arising from the solid-to-solid phase transitions amounted to $44\cdot87\,J\,K^{-1}\,mol^{-1}$. This value corresponds to $25\cdot8$ per cent of the total transition entropy ($173\cdot91\,J\,K^{-1}\,mol^{-1}$). Although the entropy gained through the phase transitions in the solid state is not so large compared with those of other discotic mesogens, the present result still strongly supports the prediction [24–26] that a rich solid polymorphism arising from the conformational melting of the alkyl-chains in the solid state is a necessary condition for the formation of columnar discotic mesophases.

In order to compare the present results more closely with those of similar discotic mesogens, we summarize available their transition entropies in table 4, in which

M. Sorai *et al.*

Table 4. Transition entropies of discotic compounds (in $J\,K^{-1}\,mol^{-1}$).

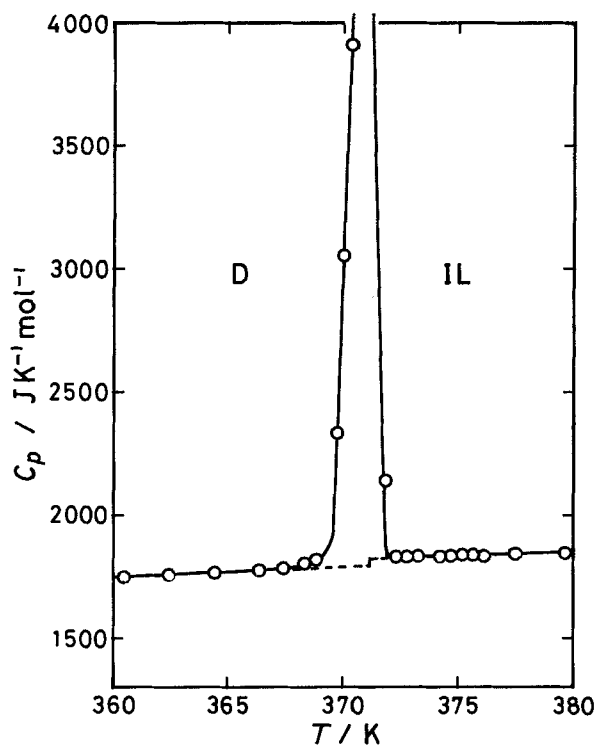| Compound	Number of transition in the solid	ΔS(solid)	ΔS(melting)	ΔS(D $\to$ IL)	ΔS(total)	Mesophase structure
BH6	3	195.46(68.3%)	90.86(31.7%)	—	286.32(100%) [22]	—
BH7	3	58.90(28.1%)	91.08(43.4%)	59.93(28.5%)	209.91(100%) [24]	Dt [14]
BH8	1	164.01(47.2%)	129.81(37.3%)	53.77(15.5%)	347.59(100%) [25]	Dt [14]
HAT-C8	4	> 85 (53%)	66.76(42%)	9.02(5%)	160.78(100%) [26]	Drd [31]
C6-HET	5	44.87(25.8%)	114.91(66.1%)	14.13(8.1%)	173.91(100%)	Dho [17]

Figure 7. Molar heat capacity of C6-HET in the vicinity of the phase transition from the columnar mesophase (D) to isotropic liquid (IL). The broken line stands for the normal heat capacity.

BHn (n = 6, 7, 8) have benzene cores while HAT-C8 and C6-HET have triphenylene cores. Clearly there exist systematic differences between the benzene and triphenylene derivatives.

First, the transition entropy gained through the solid state phase transitions is generally larger for the disc-shaped compounds having a benzene core than for those having a triphenylene core. In particular, this is obvious when C6-HET is compared with BH6 whose side chain contains the same number of carbon atoms as C6-HET. Similarly, HAT-C8 can be compared with BH8 where only the central triphenylene core is replaced by a benzene core.

Second, the entropy acquisition due to the phase transition from the columnar mesophase to the isotropic liquid is remarkably larger for the benzene derivatives (54 $\sim$ 60 J K^{-1} mol^{-1}) than for the triphenylene derivatives (9 $\sim$ 14 J K^{-1} mol^{-1}). In other words, molecular conformations in the columnar mesophase of the triphenylene derivatives are more dynamic and highly disordered in comparison with those of the benzene derivatives at the same relative temperature. Spectroscopic studies based on ^{1}H N.M.R. [35, 36], ^{2}H N.M.R. [37–40] and ^{13}C N.M.R. [41] for the Cn-HET homologous series have revealed dynamic disordering of the alkyl-chains in their columnar mesophases.

Third, the total transition entropy is much greater for the benzene derivatives (210 $\sim$ 348 J K^{-1} mol^{-1}) than for the triphenylene derivatives (161 $\sim$ 174 J K^{-1} mol^{-1}).

In order better to observe the effect of increased molecular chain conformations in terms of molar entropy, we plotted in figure 8 the molar entropies divided by
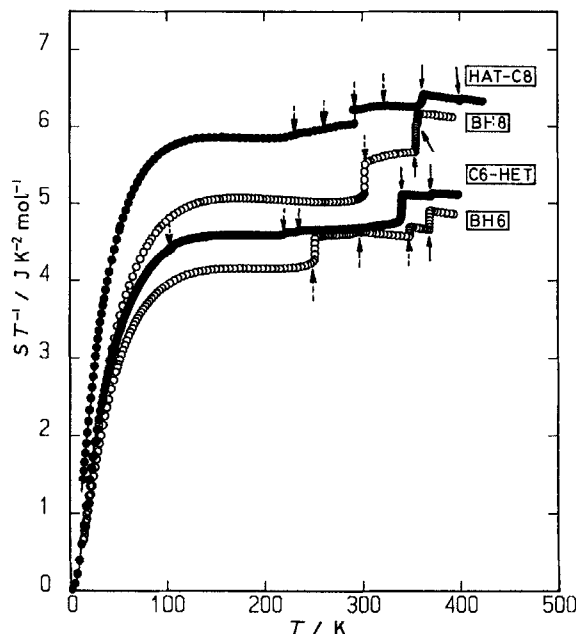
Figure 8.   Plots for the tempered entropies (molar entropies divided by temperature) against temperature for BH6, BH8, HAT-C8, and C6-HET. Two solid line arrows attached to the curves for BH8, HAT-C8, and C6-HET indicate the melting and clearing points while a solid arrow of BH6 corresponds to the melting point. The broken line arrows of respective curves shows the temperatures at which the solid-to-solid phase transitions occur.

temperature (hereafter denoted as 'tempered entropy') against temperature for BH6, BH8, C6-HET and HAT-C8. Although the coordinate is not the molar entropy itself, this kind of plot is very convenient to compare the magnitude of the molar entropy among various compounds at a given temperature and to overlook the gross aspect of temperature dependence of the molar entropy. The entropy changes are possible two ways: one is a cooperative excitation accompanied by a phase transition and the other is a noncooperative disordering without any phase transitions. A first-order phase transition with a large entropy gain corresponds to a vertical change in a curve of the tempered entropy while a higher-order phase transition with a small entropy gain appears as a wedge.

    According to the number of carbon atoms in a side-chain, C6-HET should be favourably compared with BH6 while HAT-C8 with BH8. Since the triphenylene core is massive compared with the benzene core, the tempered entropy of the triphenylene derivative should be somewhat larger than that of the benzene derivative even if their side-chains are identical. Beyond this discrepancy, however, figure 8 reveals remarkably different temperature-dependence of the molar entropies between the benzene and triphenylene derivatives. In the solid state the tempered entropy curves for the triphenylene derivatives are 'smooth' compared with those for the benzene derivatives. Moreover, the absolute value of the former is much larger than the latter at all temperatures in the solid state. This fact indicates that the conformational melting of the alkyl-chains does proceed more cooperatively through big phase transitions in the benzene derivatives than in the triphenylene derivatives. An explanation of this observation is suggested from the molecular arrangements in the crystalline state elucidated by X-ray diffraction [42] and semi-empirical calculations [43, 44]

for the HAT-Cn and Cn-HET series. These disc-shaped molecules give either irregular columns, resulting in piled pairs of neighbouring aromatic cores, or regular columns of helicoidal type. Although such studies have not been made for the BHn homologous series, it is very likely that the benzene hexa-esters might have similar molecular conformation and arrangement in the crystalline state. If this is the case, intermolecular distances between the alkyl-chains belonging to neighbouring columns would be longer for the triphenylene derivatives than for the benzene derivatives because the column size of the former is greater than that of the latter. The alkyl-chains of the triphenylene derivatives, therefore, sense weaker intermolecular and intramolecular potentials and easily undergo conformational changes in the solid state. This would reduce the cooperative nature for the conformational melting of the alkyl-chains in the triphenylene derivatives.

If the alkyl-chains make frequent conformational changes of the gauche-trans type, the rigid side-chains become flexible and consequently the core distances would be reduced. If this is the case, the columnar structure characteristic of the discotic mesophase already exists, at least to some extent, in the crystalline state. Thus the possibility of conformational chain melting is a favorable factor for formation of the columnar structure in the discotic mesophase.

4.2. *Small heat capacity of the columnar mesophase*

As described in §3, the heat capacity of the columnar mesophase is smaller than those of the adjacent crystalline and isotropic liquid phases. The heat capacity is lowered about $80\,J\,K^{-1}\,mol^{-1}$ on going from Phase I to the mesomorphic phase while it is raised about $28\,J\,K^{-1}\,mol^{-1}$ by the mesophase-to-liquid transition. This is a common tendency observed for all discotic mesogens [24–26]. In view of the fact that classical rod-like liquid crystals have always larger heat capacity in their mesophases than in the adjacent solid and liquid phases [45–53], this feature seems to be one of the essential characteristics of the columnar mesophase.

A possible origin for the mesophase heat capacity lower than the solid phase may arise from excitations in rotational-vibration modes of the alkyl moieties. A one-dimensional rotator is known to exhibit a heat-capacity maximum of the order of the gas constant, R, in the temperature region where the thermal energy is comparable with its potential barrier, while the heat capacity approaches $R/2$ in the limit of a free-rotator [54]. In the discotic mesogens, the successive conformational melting of the alkyl-chains is proceeded to a great extent through a rich solid polymorphism. Consequently, the rotational–vibrational motions of the methylene and methyl groups in an alkyl-chain are well excited even in the solid state. In the columnar mesophase, these motions are further excited to a free-rotator and hence the heat capacity is reduced at the melting point.

The larger heat capacity of the isotropic liquid compared to the columnar mesophase, on the other hand, may be attributed to both excitations of translational modes and volumetric effect due to thermal expansion at the clearing point [55].

4.3. *Temperature range of columnar mesophase*

An important factor for disc-shaped compounds to exhibit a thermally stable columnar mesophase persisting over a sizeable temperature range is obviously the intermolecular forces connecting the central aromatic cores. The discotic mesogens having a benzene core (BH7, BH8) exhibit the columnar mesophase only for an interval of 2 ~ 6 K whereas those having a triphenylene core (HAT-C8, C6-HET)

can exhibit the mesophase over $31 \sim 40\,K$. Since the triphenylene core forms a bigger π-electron system than the benzene core, van der Waals interaction between the cores is stronger. The dipole–dipole interaction between the bond moments locally existing in the molecules and intermolecular hydrogen bonding [20] are also important and serve as a 'fastener' effect. In fact, when the $-OCOC_nH_{2n+1}$ side-chains of the BHn homologous series are partially replaced by $-NHCOC_nH_{2n+1}$ groups having strong bond moment [19] and capability of forming the intermolecular hydrogen bonding, the intermolecular interactions within columns are strengthened and the temperature range for the mesophase is dramatically extended to $\sim 140\,K$ [21].

When the mesophase persists over a wide temperature range, thermal motion of the side-chains is inevitably different between the initial and final stages in a given columnar mesophase. The degree of the thermal motion in the mesophase near the clearing point is very close to that in the isotropic liquid. This is the reason why the entropy gain at the clearing point is much less for the triphenylene derivatives than for the benzene derivatives (see table 4). Moreover, small heat capacity jump of C6-HET at the clearing point compared with BH7 [24] and BH8 [25] can be explained along the same reason.

It should be finally remarked that Kohne and Praefcke [56–58] have reported that when the benzene core of the BHn series are replaced by *scyllo*-inositol the resulting mesogens exhibit a wide mesophase region of $\sim 130\,K$. Since *scyllo*-inositol is a non-aromatic and non-planar molecule, the intermolecular forces binding the neighboring cores could be neither simple van der Waals interactions arising from aromatic system nor the dipole–dipole interactions between the bond moments. In addition, the *scyllo*-inositol derivatives are unable to form the intermolecular hydrogen bonding. In this regard, detailed studies to elucidate the origin of the thermal stability of these mesogens including calorimetric study are of great interest.

References

[1] CHANDRASEKHAR, S. SADASHIVA, B. K., and SURESH, K. A., 1977, *Pramana*, **9**, 471.
[2] NGUYEN, H. T., DUBOIS, J. C., MALTHÊTE, J., and DESTRADE, C., 1978, *C. r. hebd. Séanc. Acad. Sci., Paris*, **286**, C463.
[3] BILLARD, J., DUBOIS, J. C., NGUYEN, H. T., and ZANN, A., 1978, *Nouv. J. Chim.*, **2**, 535.
[4] DESTRADE, C., MONDON, M. C., and MALTHÊTE, J., 1979, *J. Phys. Paris*, **40**, C3-17.
[5] CHANDRASEKHAR, S., SADASHIVA, B. K., SURESH, K. A., MADHUSUDANA, N. V., KUMAR, S., SHASHIDHAR, R., and VENKATESH, G., 1979, *J. Phys. Paris*, **40**, C3-120.
[6] BILLARD, J., 1980, *Liquid Crystals of One- and Two-Dimensional Order*, edited by W. Helfrich and G. Heppke (Springer), p. 383.
[7] DESTRADE, C., MALTHÊTE, J., NGUYEN, H. T., and GASPAROUX, H., 1980, *Physics Lett.* A, **78**, 82.
[8] CHANDRASEKHAR, S., 1981, *Molec. Crystals liq. Crystals*, **63**, 171.
[9] DESTRADE, C., NGUYEN, H. T., GASPAROUX, H., MALTHÊTE, J., and LEVELUT, A. M., 1981, *Molec. Crystals liq. Crystals*, **71**, 111.

[10] CHANDRASEKHAR, S., 1982, *Advances in Liquid Crystals*, Vol. 5, edited by G. H. Brown (Academic Press), p. 47.

[11] LEVELUT, A. M., 1983, *J. Chim. phys.*, **80**, 149.

[12] DESTRADE, C., GASPAROUX, H., FOUCHER, P., NGUYEN, H. T., MALTHÊTE, J., and JACQUES, J., 1983, *J. Chim. phys.*, **80**, 137.

[13] DUBOIS, J. C., and BILLARD, J., 1984, *Liquid Crystals and Ordered Fluids*, Vol. 4, edited by A. C. Griffin and J. E. Johnson (Plenum Press), p. 1043.

[14] DESTRADE, C., FOUCHER, P., GASPAROUX, H., NGUYEN, H. T., LEVELUT, A. M., and MALTHÊTE, J., 1984, *Molec. Crystals liq. Crystals*, **106**, 121.

[15] NGUYEN, H. T., DESTRATE, C., and GASPAROUX, H., 1979, *Physics Lett.* A, **72**, 251.

[16] DESTRADE, C., NGUYEN, H. T., MALTHÊTE, J., and JACQUES, J., 1980, *Physics Lett.* A, **79**, 189.

[17] LEVELUT, A. M., 1979, *J. Phys., Paris*, **40**, L-81.

[18] SMITH, G. W., 1980, *Molec. Crystals liq. Crystals*, **64**, L-15.

[19] SMITH, J. W., 1955, *Electronic Dipole Moments* (Butterworths Scientific Publications).

[20] GRAY, G. W., 1974, *Liquid Crystals and Plastic Crystals*, Vol. 1, edited by G. W. Gray and P. A. Winsor (Ellis Horwood Limited), Chap. 4.

[21] KOBAYASHI, Y., and MATSUNAGA, Y., 1987, *Bull. chem. Soc. Japan*, **60**, 3515.

[22] SORAI, M., TSUJI, K., SUGA, H., and SEKI, S., 1980, *Molec. Crystals liq. Crystals*, **59**, 33.

[23] SORAI, M., TSUJI, K., SUGA, H., and SEKI, S., 1980, *Liquid Crystals*, edited by S. Chandrasekhar (Heyden), p. 41.

[24] SORAI, M., and SUGA, H., 1981, *Molec. Crystals liq. Crystals*, **73**, 47.

[25] SORAI, M., YOSHIOKA, H., and SUGA, H., 1982, *Molec. Crystals liq. Crystals*, **84**, 39.

[26] VAN HECKE, G. R., KAJI, K., and SORAI, M., 1986, *Molec. Crystals liq. Crystals*, **136**, 197.

[27] LIFSHITZ, E., GOLDFARB, D., VEGA, S., LUX, Z., and ZIMMERMANN, H., 1987, *J. Am. chem. Soc.*, **109**, 7280.

[28] TORIUMI, H., SHIMMURA, T., WATANABE, H., and SAITO, H., 1988, *Bull. chem. Soc. Japan*, **61**, 2569.

[29] KHETRAPAL, C. L., RAGHOTHAMA, S., SURYAPRAKASH, N., and KUNWAR, A. C., 1988, *Liq. Crystals*, **3**, 413.

[30] SORAI, M., and KAJI, K., *Construction of an Adiabatic Calorimeter Capable of Measuring Heat-capacity in the Range from 13 to 520 K* (unpublished).

[31] LEVELUT, A. M., 1980, *Liquid Crystals*, edited by S. Chandrasekhar (Heyden), p. 21.

[32] SORAI, M., and SEKI, S., 1972, *J. phys. Soc. Japan*, **32**, 382.

[33] YANG, X., WALDMAN, D. A., HSU, S. L., NITZSCHE, S. A., THAKUR, R., COLLARD, D. M., LILLYA, C. P., and STIDHAM, H. D., 1988, *J. chem. Phys.*, **89**, 5950.

[34] REY-LAFON, M., DESTRADE, C., and TAZI-HEMIDA, A., 1986, *Molec. Crystals liq. Crystals*, **137**, 381.

[35] MARTINS, A. F., and RIBEIRO, A. C., 1980, *Portugal Phys.*, **11**, 169.

[36] VILFAN, M., LAHAJNAR, G., RUTAR, V., BLINC, R., TOPIC, B., ZANN, A., and DUBOIS, J. C., 1981, *J. chem. Phys.*, **75**, 5250.

[37] GOLDFARB, D., LUZ, Z., and ZIMMERMANN, H., 1981, *J. Phys., Paris*, **42**, 1303.

[38] GOLDFARB, D., LUZ, Z., and ZIMMERMANN, H., 1983, *J. chem. Phys.*, **78**, 7065.

[39] SAMULSKI, E. T., and TORIUMI, H., 1983, *J. chem. Phys.*, **79**, 5194.

[40] GOLDFARB, D., LUZ, Z., and ZIMMERMANN, H., 1983, *Israel J. Chem.*, **23**, 341.

[41] RUTAR, V., BLINC, R., VILFAN, M., ZANN, A., and DUBOIS, J. C., 1982, *J. Phys., Paris*, **43**, 761.

[42] COTRAIT, M., MARSAU, P., DESTRADE, C., and MALTHÊTE, J., 1979, *J. Phys., Paris*, **40**, L-519.

[43] PESQUER, M., COTRAIT, M., MARSAU, P., and VOLPILHAC, V., 1980, *J. Phys., Paris*, **41**, 1039.

[44] COTRAIT, M., MARSAU, P., PESQUER, M., and VOLPILHAC, V., 1982, *J. Phys., Paris*, **43**, 355.

[45] ARNOLD, H., and ROEDIGER, P., 1968, *Z. phys. Chem.*, **239**, 283.

[46] ARNOLD, H., JACOBS, J., and SONNTAG, O., 1969, *Z. phys. Chem.*, **240**, 177.

[47] SORAI, M., and SEKI, S., 1973, *Molec. Crystals liq. Crystals*, **23**, 299.

[48] SORAI, M., NAKAMURA, T., and SEKI, S., 1974, *Bull. chem. Soc. Japan*, **47**, 2192.

[49] TSUJI, K., SORAI, M., SUGA, H., and SEKI, S., 1977, *Molec. Crystals liq. Crystals*, **41**, L-81.

[50] TSUJI, K., SORAI, M., SUGA, H., and SEKI, S., 1979, *Molec. Crystals liq. Crystals*, **55**, 71.

[51] TSUJI, K., SORAI, M., SUGA, H., and SEKI, S., 1982, *Molec. Crystals liq. Crystals*, **87**, 293.

[52] TSUJI, K., SORAI, M., SUGA, H., and SEKI, S., 1982, *Molec. Crystals liq. Crystals*, **87**, 305.
[53] TSUJI, K., SORAI, M., SUGA, H., and SEKI, S., 1982, *Molec. Crystals liq. Crystals*, **90**, 97.
[54] PITZER, K. S., and GWINN, W. D., 1942, *J. chem. Phys.*, **10**, 428.
[55] SMITH, T. H., and VAN HECKE, G. R., 1981, *Molec. Crystals liq. Crystals*, **68**, 23.
[56] KOHNE, B., and PRAEFCKE, K., 1984, *Angew. Chem. Int. Ed. Engl.*, **23**, 82.
[57] KOHNE, B., and PRAEFCKE, K., 1985, *Z. Naturf. (b)*, **40**, 981.
[58] KOHNE, B., and PRAEFCKE, K., 1986, *Z. Naturf. (b)*, **41**, 1036.